Solar Energy Materials & Solar Cells 105 (2012) 27–39

Contents lists available at SciVerse ScienceDirect

Solar Energy Materials & Solar Cells

journal homepage: www.elsevier.com/locate/solmat

On the experimental validation of an improved five-parameter model for silicon photovoltaic modules

Valerio Lo Brano*, Aldo Orioli, Giuseppina Ciulla

D.D.E. Dipartimento dell'Energia, Università degli Studi di Palermo, viale delle scienze, edificio 9, Italy

ARTICLE INFO

Article history:
Received 11 October 2011
Received in revised form
16 May 2012
Accepted 22 May 2012
Available online 15 June 2012

Keywords:
Silicon photovoltaic modules
Five-parameter model
I–V characteristics
Experimental validation
Solar energy

ABSTRACT

This paper presents the experimental validation of a new five-parameter model capable of analytically describing the I–V characteristic of a silicon photovoltaic module for each generic condition of operative temperature and solar irradiance. The operating current calculated with the model was validated on the basis of a series of experimental measurements performed in the field on two commercial silicon photovoltaic panels connected to a set of nine constant values of the electrical load. In order to examine the panels working in almost steady-state conditions only the data-sets of the sunniest days from sunrise to sunset were used.

Unfortunately the production spread of photovoltaic panels did not permit the consistent comparison between the measurements and the data calculated by the model on the basis of the electrical characteristics provided by the manufactures. To surmount such an obstacle the determination of the particular current–voltage characteristic of the tested photovoltaic panel specimens was successfully attempted by filtering the collected data. The results of comparison have shown that the model defined by the new electrical characteristics is able to evaluate the operating current with a high degree of accuracy, even during days perturbed by very variable conditions of solar irradiance.

1. Introduction

The success of any new technology depends on the ability to demonstrate its actual advantages. Because there is no direct experience with its application, the effectiveness of a new technology is often assessed on the basis of the results obtained from predictive performance tools. A good predictive tool should allow the designer to optimise the performance and maximise the cost-effectiveness of a system before installation. This optimisation is especially significant in the field of renewable energy systems because their effectiveness is usually affected by many erratic physical parameters.

The accurate and reliable assessment of PV system performance incorporates many important features. Some attributes can be determined precisely, including site latitude, tilt and azimuth angles of the panel and the effects of shading obstructions; other aspects such as solar energy, air temperature, wind speed, temperature of the surrounding surfaces and electrical load can vary over time and can only be estimated. All of these features strongly affect the conversion efficiency, which is the most important parameter of a PV module.

Unfortunately, the data issued by the manufacturers of PV modules do not help us to determine the conversion efficiency because they relate only to the fixed standard conditions of solar irradiance and operating temperature. Many researchers have therefore agreed that it is important to find and validate reliable models for predicting the electrical performance of the PV panel when solar irradiance, electrical load and operating temperature do not correspond to the standard test conditions (STC). Nowadays many effective models are available [1–5]. These models are capable of accurately describing the electrical behaviour of a PV panel by using the information contained in the I–V characteristics, which are supposed to be obtained from accurate laboratory measurements.

Due to the number of parameters affecting the physical behaviour, the experimental validation of a PV panel model requires a great amount of measurements that can be taken outside or inside a laboratory. The data collected in the field take into account of more realistic conditions; such measurements are very long and cannot be scheduled because it is obviously impossible to control the proper atmospheric conditions. On the other hand, compared with laboratory tests, the outside measurements give more information since they are sensitive of important features, like the reflexion and the absorption of the solar radiation at non-normal and variable incidence angles or the non-uniform temperature distribution across the panel.

* Corresponding author
E-mail address: lobrano@dream.unipa.it (V. Lo Brano).

0927-0248/$ - see front matter © 2012 Elsevier B.V. All rights reserved.
http://dx.doi.org/10.1016/j.solmat.2012.05.028

Nomenclature

AM	air mass
AM_a	absolute air mass
G	solar irradiance [W/m^2]
G_{ref}	solar irradiance at STC (1000 W/m^2)
I	current generated by the panel [A]
I_L	photocurrent [A]
$I_{L,\text{ref}}$	photocurrent at STC [A]
I^*_{mp}	current at the maximum power point with $T \neq 25$ °C and $G=G_{\text{ref}}$ [A]
I_{mp}	current at the maximum power point [A]
I_{sc}	short circuit current [A]
$I_{sc,\text{ref}}$	short circuit current at STC [A]
I_0	reverse saturation current [A]
k	Boltzmann constant [J/K]
K	thermal correction factor [Ω/°C]
h	site altitude [m]
n	diode quality factor
N_{cs}	number of cells connected in series
q	electron charge [C]
R_L	electrical load [Ω]
R_s	series resistance [Ω]
R_{sh}	shunt resistance [Ω]
T	temperature of the PV cell [°K]
T_{ref}	temperature of the panel at STC (25 °C–298.15 °K)
V	voltage generated by the PV panel [V]
V^*_{mp}	voltage at the maximum power point with $T \neq 25$ °C and $G=G_{\text{ref}}$ [V]
V_{oc}	open circuit voltage of the panel [V]
Z_s	solar zenith angle [°]
α_G	ratio between the current irradiance and the irradiance at STC
γ	ideality factor
$\mu_{I,sc}$	thermal coefficient of the short circuit current [A/°C]
$\mu_{V,oc}$	thermal coefficient of the open circuit voltage [V/°C]

The results of the experimental validation of the five-parameter model of Lo Brano et al. [6], which was performed on mono-crystalline and polycrystalline silicon PV modules, are described in this paper.

2. The equivalent electrical circuit of the PV module

The physical behaviour of a PV panel has traditionally been studied by representing it as an equivalent electrical circuit composed of linear and non-linear components. The parameters describing these components are directly related to the performance characteristics of the specific PV panel, which are generally available in graphic form with respect to standard values of temperature and incident radiation. Wolf [7] proposed a simplified equivalent circuit containing two diodes, a current generator and two resistors; the resistors are used to describe the dissipative effects that are mainly due to the electrical contact between the electrodes and silicon and to account for the presence of any by-passing currents caused by construction defects. The model requires the determination of seven parameters, which variously affect the shape of the I–V characteristic. Specifically, the resistances change the slope of the I–V characteristic before and after the knee of the curve, and the ratio of the reverse saturation currents of the diodes affects the bend curvature [8]. As a consequence of recent technological research, modern mono-crystalline and polycrystalline silicon PV panels have a good fill factor and therefore an I–V characteristic with a very sharp bend. This characteristic can be effectively reproduced by the one-diode equivalent circuit shown in Fig. 1.

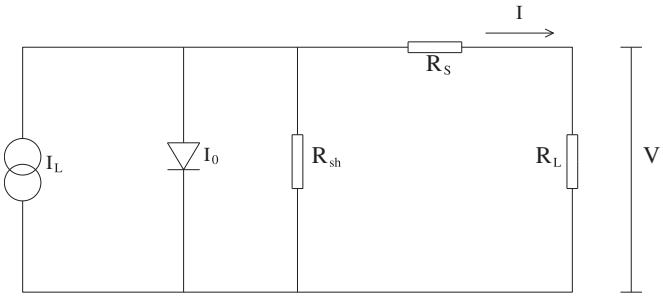

Fig. 1. One-diode equivalent circuit for a PV panel.

The equivalent circuit is described by the following five-parameter equation:

$$I = I_L - I_0\left(e^{(V+IR_s/nT)}-1\right) - \frac{V+IR_s}{R_{sh}} \tag{1}$$

where following traditional theory, the photocurrent I_L depends on solar irradiance, the reverse saturation current I_0 is affected by silicon temperature and n, R_s and R_{sh} are constant.

Lo Brano et al. [6] have proposed Eq. 4, which better represents the electrical and thermal behaviour of a PV panel than Eq. 1:

$$I(\alpha_G,T) = \alpha_G I_L(T) - I_0(\alpha_G,T)\left(e^{\alpha_G[V+KI(T-T_{ref})]+IR_s/\alpha_G nT}-1\right) - \frac{\alpha_G[V+KI(T-T_{ref})]+IR_s}{R_{sh}} \tag{2}$$

in which T is the silicon absolute temperature and the quantity $\alpha_G=G/G_{\text{ref}}$ denotes the ratio between the generic solar irradiance and the irradiance at STC, which corresponds to an irradiance level of 1000 W/m^2, an air mass of 1.5 and a cell or module junction temperature of 25 °C. K is a thermal correction factor, similar to the curve correction factor described by IEC 891, which becomes significant when the temperature of the panel is different from the reference temperature T_{ref} at STC. The photocurrent $I_L(T)$ can be evaluated with the equation:

$$I_L(T) = I_{L,ref} + \mu_{I,sc}(T-T_{ref}) \tag{3}$$

where $I_{L,\text{ref}}$ is the value of the photocurrent at STC and $\mu_{I,sc}$ is the short circuit current temperature coefficient. The parameters n, R_s and R_{sh} are set constant in Eq. 2 for each temperature and irradiance; actually due to the presence of α_G in the exponential function and in the third term of Eq. 2, the computation of the current is affected by values of resistances that are inversely proportional to the irradiance. The current $I_0(\alpha_G,T_.)$ can be obtained by the following interpolating equation:

$$I_0(\alpha_G,T) = \exp\left[\left(\frac{\alpha_G-0.2}{1-0.2}\right)\ln\frac{I_0(1,T)}{I_0(0.2,T)} + \ln I_0(0.2,T)\right] \tag{4}$$

in which $I_0(1,T)$ and $I_0(0.2,T)$ are evaluated by means of the equation:

$$I_0(\alpha_G,T) = \alpha_G\left(\frac{I_L(T)-V_{oc}(\alpha_G,T)/R_{sh}}{e^{V_{oc}(\alpha_G,T)/nT}-1}\right) \tag{5}$$

for $G=G_{\text{ref}}$ $=1000$ W/m^2 ($\alpha_G=1$) and $G=200$ W/m^2 ($\alpha_G=0.2$), respectively.

Table 1
Data for the evaluation of the Lo Brano et al. model parameters.

Irradiance	1 kW/m^2										0.2 kW/m^2
Temperature	25 °C						75 °C		25–75 °C		25 °C
Panel type	V_{oc} [V]	I_{sc} [A]	V_{mp} [V]	I_{mp} [A]	R_{sho} [Ω]	R_{so} [Ω]	V_{mp} [V]	I_{mp} [A]	$\mu_{V,oc}$ [V/°C]	$\mu_{I,sc}$ [A/°C]	V_{oc} [V]
Kyocera KC175GHT-2	29.35	8.07	23.60	7.57	99.44	0.419	18.00	7.50	-1.07×10^{-1}	2.22×10^{-3}	27.20
Sanyo HIP-240 HDE4	43.60	7.37	34.31	7.10	3204.64	0.873	28.89	7.13	-1.09×10^{-1}	2.12×10^{-3}	40.61

Table 2
Parameters evaluated with the Lo Brano et al. model.

Irradiance	1 kW/m^2						0.2 kW/m^2
Temperature	25 °C					25–75 °C	25 °C
Panel type	I_L [A]	I_0 [A]	n [V/K]	R_{sh} [Ω]	R_s [Ω]	K [Ω/°C]	I_0 [A]
Kyocera KC175GHT-2	8.09277	9.60241×10^{-12}	3.58974×10^{-3}	90.158	0.282	1.12182×10^{-3}	1.43561×10^{-11}
Sanyo HIP-240 HDE4	7.37160	2.01236×10^{-14}	4.36097×10^{-3}	3203.944	0.696	-1.12679×10^{-3}	4.01325×10^{-14}

The Lo Brano et al. model was tested on a Kyocera 175 W polycrystalline PV panel and a Sanyo 240 W HIT (Heterojunction with Intrinsic Thin layer) PV panel using the performance data presented in Table 1.

The data of Table 1 may result slightly different from those provided by the manufacturers; actually, for sake of accuracy, some data were directly extracted from the issued I–V characteristics. Table 2 lists the parameters of the equivalent circuit obtained by applying the procedure described in Section 3.

In Figs. 2(a), (b) and 3(a), (b) the current–voltage curves evaluated with the calculated parameters are compared with the characteristics issued by manufacturers.

In the same figures are reported the current–voltage curves extracted from the data set of PVsyst [9], which is a well-known PC software package for the study, sizing, simulation and data analysis of complete PV systems. PVsyst analytically describes a PV panel by means of the following one-diode equation:

$$I = I_L - I_0\left(e^{q(V+IR_s)/N_{cs}\gamma kT} - 1\right) - \frac{V+IR_s}{R_{sh}} \tag{6}$$

The parameters I_L, I_0 and R_s are determined by solving a system of three equations that satisfy the conditions under which Eq. (6) contains the short circuit, the open circuit and any other point, close the maximum power point. The ideality factor γ is set at a reasonable level depending on the semiconductor material ($\gamma=1.30$ for Si-monocrystalline, $\gamma=1.35$ for Si-polycrystalline,) and for N_{cs}, which is the number of cells connected in series, the value provided by the manufacture is used. Resistance R_{sh}, which is assumed to be the inverse of the slope of the I–V characteristic in the neighbourhood of the short circuit point, is determined by calculating the so-called virtual maximum power point conductance $(I_{sc}-I_{mp})/V_{mp}$, corresponding to the minimum value for R_{sh}, and taking a given fraction of this quantity. Shunt resistance R_{sh} is considered to be variable with the irradiance according to the following exponential expression:

$$R_{sh}(G) = R_{sh} + [R_{sh}(0) - R_{sh}]e^{-5.5G/G_{ref}} \tag{7}$$

that was derived by observing the behaviour of all the analysed PV panels. For silicon crystalline modules, resistance $R_{sh}(0)$ is set to the default value of four times R_{sh}. Tables 3 and 4 list the absolute mean differences and RMS deviations of the current calculated with the PVsyst and the Lo Brano et al. model for constant values of irradiance and temperature.

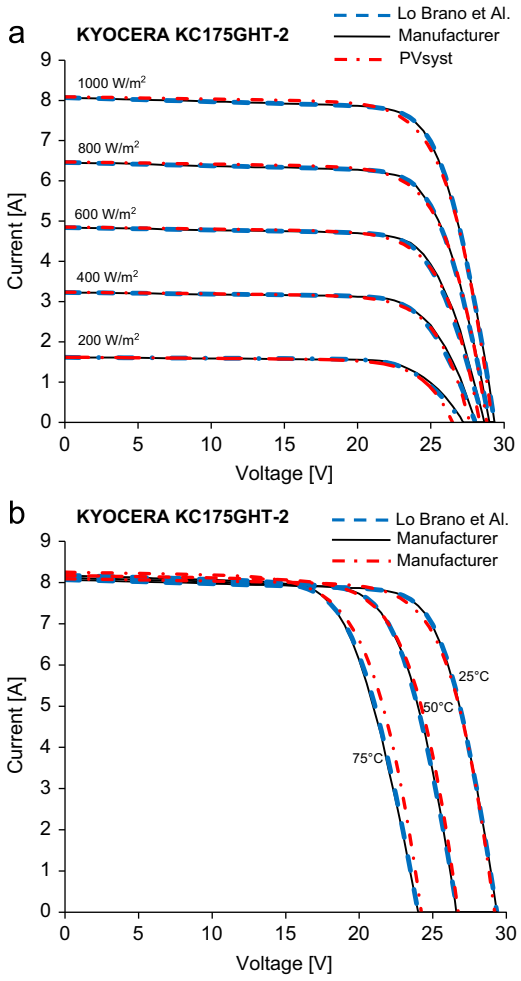

Fig. 2. (a) Comparison between calculated (Lo Brano et al. and PVsyst) and issued current–voltage characteristics of Kyocera KC175GHT-2 at temperature $T=25$ °C, using data in Tables 1 and 2. (b) Comparison between calculated (Lo Brano et al. and PVsyst) and issued current–voltage characteristics of Kyocera KC175GHT-2 at irradiance $G=1000$ W/m^2, using data in Tables 1 and 2.

Both models give an accurate representation of the I–V characteristics of the PV panels even if the Lo Brano et al. model seems to be more accurate. In Figs. 4(a), (b) and 5(a), (b) the

power–voltage curves, evaluated with the PVsyst and the Lo Brano et al. models near to maximum power points, are compared with the curves derived from the characteristics issued by manufacturers.

If models are able to accurately represent the entire I–V characteristic, they will be suitable for any general purpose. In particular the Lo Brano et al. model is very precise near the maximum power points and for this reason it may be used to simulate the functioning of PV systems provided with maximum power point trackers. Depending on the used algorithm, these very efficient devices, which are supposed to be able to maximise the PV energy collection, can be affected by oscillations and perform erratically when the irradiance is quickly changing. The capability to precisely represent the current–voltage near to the maximum power point permits to accurately predict the annual energy production even taking account of the performance of PV plants provided with imperfect maximum power point trackers.

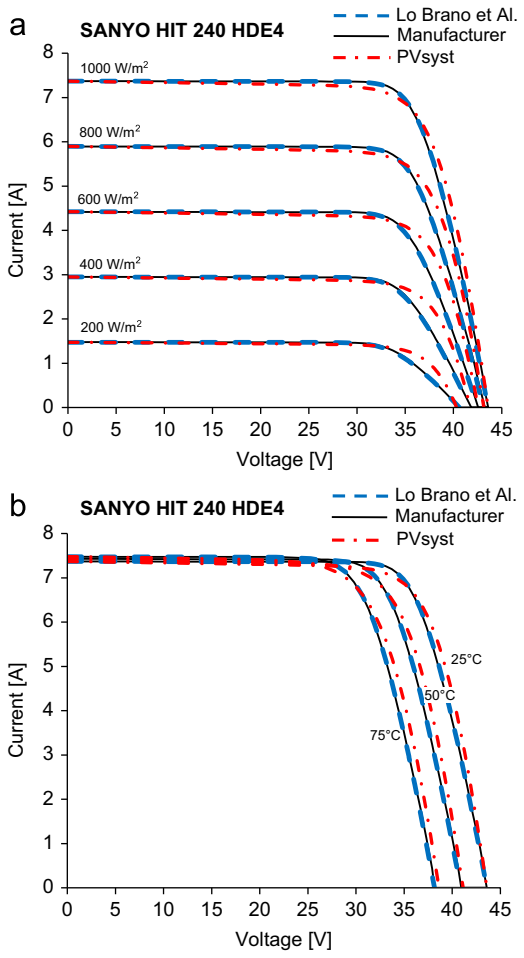

Fig. 3. (a) Comparison between calculated (Lo Brano et al. and PVsyst) and issued current–voltage characteristics of Sanyo HIT 240 HDE4 at temperature $T=25$ °C, using data in Tables 1 and 2. (b) Comparison between calculated (Lo Brano et al. and PVsyst) and issued current–voltage characteristics of Sanyo HIT 240 HDE4 at irradiance $G=1000$ W/m^2, using data in Tables 1 and 2.

3. Experimental validation of the model

Many authors have recently described their experimental studies regarding PV concentrators [10,11], PV-based water pumping installations [12,13], hybrid photovoltaic thermal collectors [14–18] and photovoltaic/heat pump systems [19–21]. Roman et al. [22] tested a system of four PV modules with their respective DC–DC converters connected in series to a PV inverter working in constant voltage mode.

Other authors more specifically aimed to the experimental validation of the models proposed to simulate the physical behaviour of PV panels. De Blas et al. [3] used a series of experimental curves related to different irradiance and temperature conditions with natural sunlight on clear days. The curves were measured using a bipolar power supply that acts as a charge on the solar module under study, the voltage of which was uniformly increased. The voltage and the current of the PV module were recorded at each operating point with two high precision meters. De Soto et al. [1] used the data provided by Fanney et al. [23] from a building integrated photovoltaic facility at the NIST in Gaithersburg, Maryland. The experimental data provided, at five-minute intervals, one year of meteorological data and measured cell temperatures along with current and voltage values of for four different photovoltaic cell technology types installed on a vertical surface. Both De Blas et al. [3] and De Soto et al. [1] compared the measured current–voltage curves with those calculated with the proposed models.

Celik and Acikgoz [4] performed the experimental verification of a couple of 120 W mono-crystalline modules mounted with a tilt angle equal to the latitude of the location (36.35 °N). The experimental system consisted of a 200 A h/12 V sealed type lead-acid battery and a DC/AC inverter of 600 W/12 V and 230 V/50 Hz, with a maximum efficiency of 98%. The PV modules were connected to the battery and to the electrical load through an inverter and a charge controller. The electrical load connected to the inverter output was a set of light bulbs, whose power was varied between 0 to 200 W depending on the state of charge of the battery. The experimental verification of the model was carried out under system real working conditions measuring the current and voltage of the PV modules. The predicted results of the operating current evaluated with the Hadj Arab et al. [5] model were analysed for five meteorological data-sets, each of

Table 3
Absolute mean differences and RMS deviations of the current at temperature $T=25$ °C.

PV panel	Model	Errors [A]	Irradiance [W/m^2]				
			200	400	600	800	1000
KC175GHT-2	PVsyst	Absolute mean difference	0.051	0.047	0.066	0.058	0.083
		RMS deviation	0.098	0.080	0.101	0.079	0.106
	Lo Brano et al.	Absolute mean difference	0.021	0.031	0.044	0.017	0.015
		RMS deviation	0.033	0.057	0.077	0.026	0.027
HIT-240 HDE4	PVsyst	Absolute mean difference	0.101	0.185	0.244	0.226	0.202
		RMS deviation	0.145	0.271	0.354	0.323	0.145
	Lo Brano et al.	Absolute mean difference	0.012	0.025	0.019	0.035	0.023
		RMS deviation	0.016	0.032	0.024	0.056	0.035

Table 4
Absolute mean differences and RMS deviations of the current at irradiance $G=1000$ W/m^2.

PV panel	Model	Errors [A]	Temperature [°C]		
			200	400	600
KC175GHT-2	PVsyst	Absolute mean difference	0.080	0.118	0.276
		RMS deviation	0.102	0.160	0.422
	Lo Brano et al.	Absolute mean difference	0.015	0.024	0.041
		RMS deviation	0.026	0.043	0.069
HIT-240 HDE4	PVsyst	Absolute mean difference	0.201	0.249	0.298
		RMS deviation	0.276	0.336	0.405
	Lo Brano et al.	Absolute mean difference	0.024	0.025	0.026
		RMS deviation	0.035	0.044	0.048

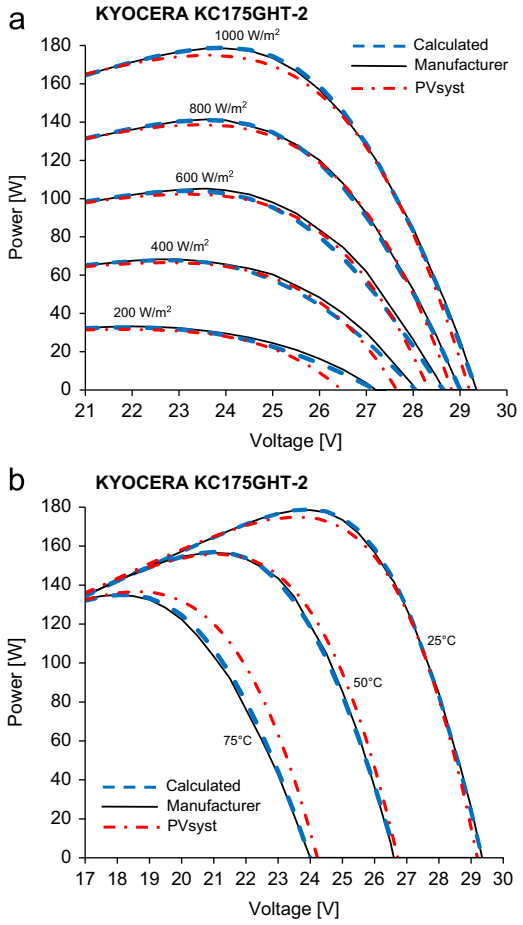

Fig. 4. (a) Comparison between calculated (Lo Brano et al. and PVsyst) and issued power–voltage characteristics of Kyocera KC175GHT-2 at temperature $T=25$ °C, using data in Tables 1 and 2. (b) Comparison between calculated (Lo Brano et al. and PVsyst) and issued power–voltage characteristics of Kyocera KC175GHT-2 at irradiance $G=1000$ W/m^2, using data in Tables 1 and 2.

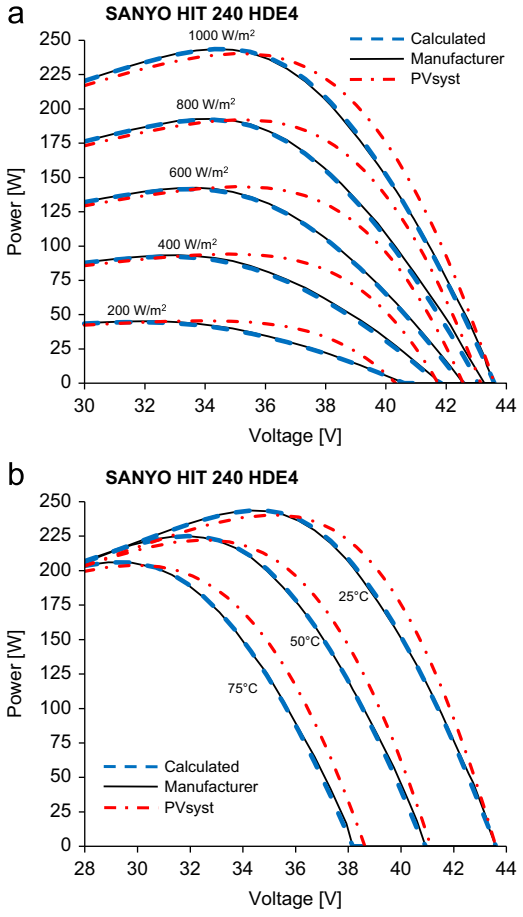

Fig. 5. (a) Comparison between calculated (Lo Brano et al. and PVsyst) and issued power–voltage characteristics of Sanyo HIT 240 HDE4 at temperature $T=25$ °C, using data in Tables 1 and 2. (b) Comparison between calculated (Lo Brano et al. and PVsyst) and issued power–voltage characteristics of Sanyo HIT 240 HDE4 at irradiance $G=1000$ W/m^2, using data in Tables 1 and 2.

them consisting of one-day long data set, from sunrise to sunset. The error in estimating the energy varied from −4.39 to 3.81% and it was observed that the calculated current differed most from the measured values around the solar noon, when the cell temperature was at its highest level during that particular day. During the measurements the maximum daily value of the cell temperature varied from 52.0 to 61.6 °C. A comparison with a four-parameter model, with an infinite shunt resistance, was made and the main conclusion was that the five-parameter model allowed more accurate current estimations.

The experimental approach of Celik and Acikgoz [4] is formally correct and well represents the way in which the panel may operate under real working conditions. Nevertheless it is sensible to wonder if the model was validated in correspondence of an appreciable number of significant working points of the I–V characteristics plane. Because a panel can operate in each of the infinite points contained in the planes of Figs. 2 and 3, the reliability of a model should be validated in correspondence of the working points that are representative of the widest set of possible conditions of irradiance and temperature.

The operating points on the I–V characteristic plane are also defined by the value of the electrical load R_L connected to the panel. For given values of irradiance, temperature and electrical load, the operating point can be determined by solving the equation system formed by the PV panel characteristic $I=f(V)$ and the electrical load characteristic $I=V/R_L$. Such a solution, if R_L

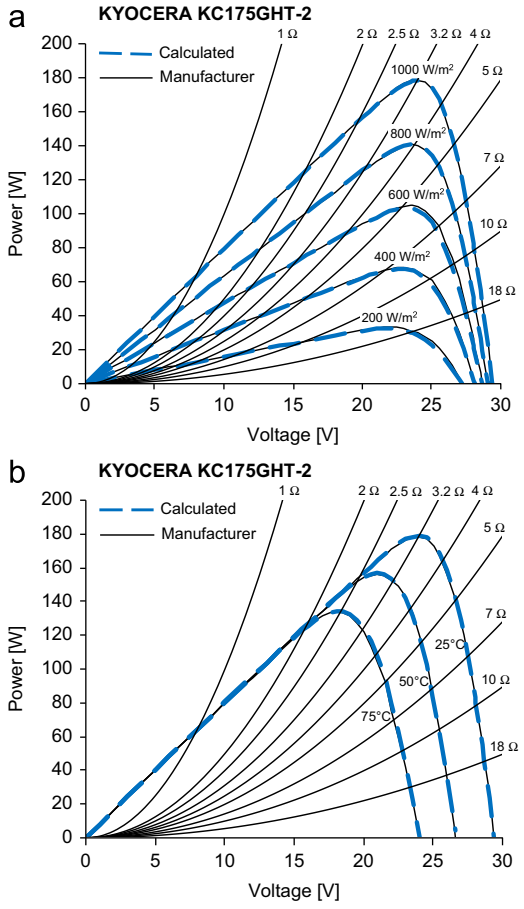

Fig. 6. (a) Electrical load, calculated and issued power–voltage characteristics of Kyocera KC175GHT-2 at temperature $T=25$ °C. (b) Electrical load, calculated and issued power–voltage characteristics of Kyocera KC175GHT-2 at irradiance $G=1000$ W/m^2.

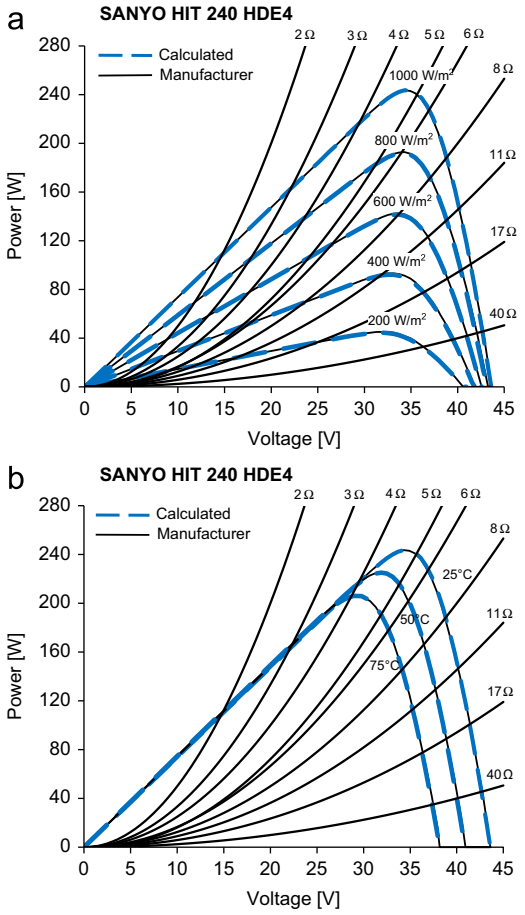

Fig. 7. (a) Electrical load, calculated and issued power–voltage characteristics of Sanyo HIT 240 HDE4 at temperature T=25 °C. (b) Electrical load, calculated and issued power–voltage characteristics of Sanyo HIT 240 HDE4 at irradiance $G=1000$ W/m^2.

is constant, can be easily achieved with a graphical method by drawing a straight line with a slope inversely proportional to R_L on the I–V characteristic plane. The intersection of the straight line and the PV panel characteristic corresponds to the working point sought. The same method can be used to draw the curve of the electrical load power $P=V^2/R_L$ on the power–voltage characteristics plane. In Figs. 6(a), (b) and 7(a), (b) the electrical load, the calculated and the issued power–voltage characteristics of Kyocera and Sanyo PV panels are shown.

The constant electrical load R_L will force the PV panel to work at operating points that are on the power–voltage characteristic corresponding to the chosen value of R_L. That curve will be travelled up and down because the operating point position will also depend on the current values of the irradiance and temperature. If a sufficient number of electrical loads are properly selected, it is possible to explore the entire area of the I–V characteristic plane and perform a significant validation of the model.

Because in the experimental system used by Celik et al. the PV panels were connected to a controller which automatically and independently performed the task of keeping the best state of charge of the battery, it was not possible to set the value of the electrical load in order to investigate the agreement between measured and calculated values in correspondence of any region of the electrical characteristics. Actually, the electrical load was continuously changing because the controller allowed the current to flow from the panel only if the battery needed to be charged. Because the connected electrical load and, consequently, the PV panel operating point were unknown, the conclusions derived by the experimental validation performed by Celik et al. may not have a general validity as they were not based on an exhaustive exploration of the electrical characteristic of the PV panel.

In order to verify the reliability of the model, the experimental apparatus should be simplified. The presence of an inverter, a charge regulator, a battery set or a time-changing electrical load, does not increase the information; on the contrary such a complex facility may make it more complicated to get a clear interpretation of the comparison between measured and calculated data. This is the reason why in this paper the experimental validation was performed simply connecting the PV panel to an electrical resistance, selected for its high stability and precision. The values of the resistances, which are indicated in Figs. 6(a), (b), 7(a), (b), were selected with the aim of performing a scanning of the I–V characteristics as regularly as possible.

To perform the measurements a simple experimental system was designed. The system was situated on the roof of the D.D.E. in Palermo (38°07′N, 13°22′E) and consisted of two silicon panels (Kyocera KC175GHT-2 and Sanyo HIT 240 HDE4) connected with a precision resistance set. The measurements were performed with a data acquisition module National Instruments NI USB-9221 and a Delta Ohm pyranometer mod. LP PYRA 02 AV, a first class according to ISO 9060, linked to an Advantech ADAM 6024 module. A Davis Vantage PRO2 Plus Weather station was used to collect the measurements of air temperature and relative humidity, wind speed and direction, horizontal global solar irradiance and atmospheric pressure.

The PV panels and the pyranometer were tilted at an angle that is equal to the latitude of the location. The values of R_L were

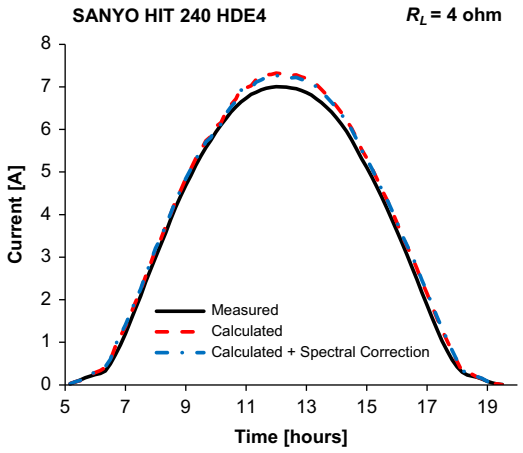

Fig. 8. Current of the PV module Sanyo HIT 240 HDE4 measured with an electrical load of 4 Ω on August 2, 2010 versus the current calculated with the Lo Brano et al. model.

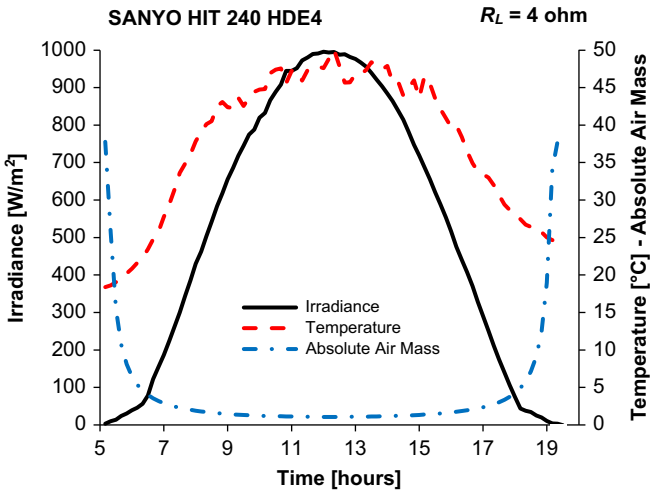

Fig. 9. Irradiance, absolute air mass and PV panel temperature on August 2, 2010.

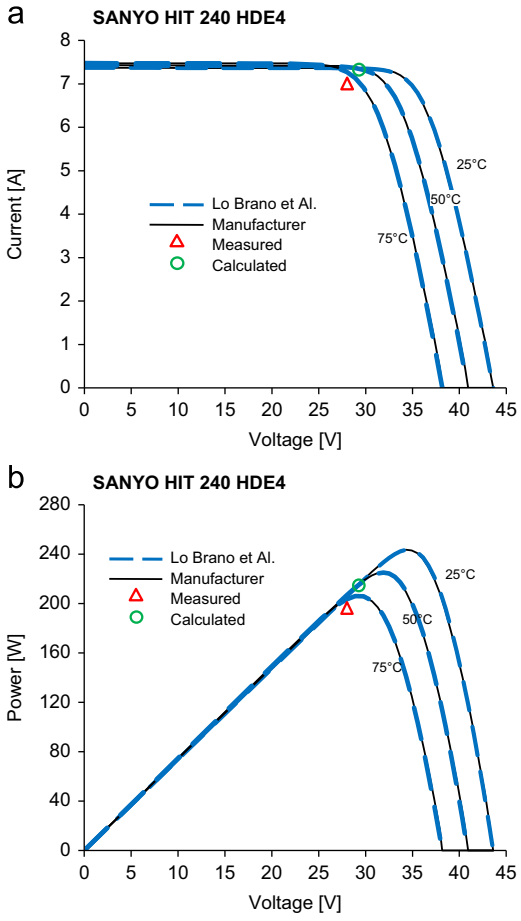

Fig. 10. (a) Comparison between the calculated and measured current values at 12:00 in the current–voltage plane of Sanyo HIT 240 HDE4 at irradiance $G=1000$ W/m^2. (b) Comparison between the calculated and measured power values at 12:00 in the power–voltage plane of Sanyo HIT 240 HDE4 at irradiance $G=1000$ W/m^2.

obtained by the parallel and/or series compositions of 3 and 4 Ω precision resistances (Vishay RH250); the values of the resistances are declared with a tolerance of ±1% and a temperature coefficient of ±50 ppm/°C. Because the resistances never exceeded a temperature of 150 °C, their nominal values were considered certain within the precision of ±1.625%. To avoid that, especially with the lowest values of R_L, the series resistance due to internal shunt of the ammeter changed the value of the electrical load connected to the PV panel, the current was not registered but calculated on the basis of the measured voltage accepting the error due to the resistance precision. The temperature of the panels was measured using some thermocouples (type T, copper-constantan) put in three different points of each panel. To get a satisfactory thermal contact with the back face of the silicon cells, the thermocouples were installed into some little holes that were made melting the rear PET (Polyethylene terephthalate) film of the panels. As it was predictable, due to the temperature gradient related to the heat transmission across the PV modules, the sensors measured slightly different values (within a 0.5 °C range); therefore the averaged values of temperature were used. The measurements were performed from April 2010 to June 2011 collecting the data every 20 s.

To assess the reliability of the model the current and power differences between calculated and measured data were evaluated. Because the model almost perfectly reproduces the I–V characteristics of the PV panels, it was expected that the differences between calculated and measured were very small; surprisingly, for some value of R_L such a difference resulted greater than that expected. The greatest differences were observed for the Sanyo panel.

As it is shown in Fig. 8, the values of current calculated for the Sanyo Panel systematically exceed the measured ones. In particular, with a load resistance of 4 Ω, the difference between calculated and measured data is 0.32 A at 12:00 when an irradiance of 996 W/m^2 and a panel temperature of 47.6 °C were measured (Fig. 9).

Such a possibility was not unexpected because it is well known that the technology of silicon devices does not permit to keep a small production spread; in particular, for the Sanyo panel an output power tolerance of −5/+10% is officially declared by the manufacturer. However, the observed power difference, which is −9.3%, is considerably greater than the value of −5% declared by the manufacturer for the maximum power.

Actually, if the issued performance data do not correspond to the actual characteristics of the tested specimen, the simulation model will be never able to accurately represent the physical behaviour of the analysed PV panel; this problem may be less evident dealing with a large PV array because the average performance of modules should be closer to the manufacturer's specification. The nominal STC current–voltage characteristics (at a constant irradiance and at a constant temperature) of the tested PV module specimen should be measured in order to get the data necessary to calculate the parameters for the simulation model. Obviously the measurements should be carried out in a laboratory for PV module performance

Table 5
Measurement uncertainties.

Instrument	Quantity	Estimate	Standard uncertainty	Probability distribution		Sensitivity coefficient	Uncertainty contribution
LP PYRA 02	Irradiance	4.96 V	0.0500	N	2.00	201 W/m^2 V	24.924 W/m^2
ADAM-6024	Voltage	4.96 V	0.0010	R	1.73	201 W/m^2 V	0.576 W/m^2
	Span drift	15.0 °C		R	1.73	$5.025 \cdot 10^{-3}$ W/m^2 V °C	0.044 W/m^2
	Zero drift	20.0 °C		R	1.73	$1.266 \cdot 10^{-3}$ W/m^2 V °C	0.015 W/m^2
Solar irradiance G=996 W/m^2						Combined uncertainty	24.931 W/m^2
						Expanded uncertainty	49.861 W/m^2
							5.006%
Thermocouple type T	Temperature	47.6 °C	0.0100	R	1.73	1	0.27482 °C
ADAM-6018	Temperature	47.6 °C	0.0010	R	1.73	1	0.02748 °C
	Span drift	15.0 °C		R	1.73	2.500×10^{-5}	0.00022 °C
	Zero drift	20.0 °C		R	1.73	6.000×10^{-7}	0.00001 °C
PV panel temperature T=47.6 °C						Combined uncertainty	0.27619 °C
						Expanded uncertainty	0.55238 °C
							1.160%
VISHAY RH250	Resistance	4.0 Ω	0.0100	R	1.73	1	0.0231 Ω
	Temp.coeff.	125.0 °C		R	1.73	5.00×10^{-5}	0.0036 Ω
Load resistance R_L=4 Ω						Combined uncertainty	0.0234 Ω
						Expanded uncertainty	0.0467 Ω
							1.169%
N.I. USB-9221	Voltage	28.03 V	0.0025	R	1.73	1	0.0405 V
	Offset	60.00 V	0.0025	R	1.73	1	0.0866 V
PV panel voltage V=28.03 V						Combined uncertainty	0.0956 V
						Expanded uncertainty	0.1912 V
							0.682%
Power=V^2/R_L	Voltage	28.03 V	0.0956 V			14.015 W/V	1.3396 W
	Resistance	4.00 Ω	0.0234 Ω			−49.105 W/Ω	−1.1478 W
PV panel power P=196.42 W						Combined uncertainty	1.7641 W
						Expanded uncertainty	3.5282 W
							1.796%
Current=V/R_L	Voltage	28.03 V	0.0956 V			0.250 A/V	0.0239 A
	Resistance	4.00 Ω	0.0234 Ω			−1.752 A/Ω	−0.0409 A
PV panel current I=7.008 A						Combined uncertainty	0.0474 A
						Expanded uncertainty	0.0948 A
							1.353%

testing in order to keep the constant values of solar irradiance and silicon temperature that are necessary to draw the the nominal STC current–voltage characteristics of the tested specimen of PV panel.

In the outside measurements the only possibility to get an almost constant irradiance, during the response time of the pyranometer, is given by the use of perfect cloudless days, which seldom occur, even in summer, in a sunny place like Sicily. In order to estimate the uncertainties in testing, a very large amount of measurements should be taken on the tested specimen following the measurement good practice. Dealing with the sun it is quite impossible to measure the complete I–V curve for constant values of irradiance and temperature.

Fig. 10 permit to visually appreciate the difference between the above couple of measured and calculated data. The curves are referred to an irradiance of 1000 W/m^2, which is only 0.4% greater than the measured value; the middle curves refer to a temperature of 50 °C that is 5% greater than the measured one.

It can be observed that the data of the calculated current and power are extremely close to the curve corresponding to 50 °C even if the temperature of the PV panel is 5% less than 50 °C. Actually, because the operating point indicated by the small circle is located in the flat part of the current–voltage characteristic, the PV current mainly depends on the solar irradiance. The measured data (small triangles) are situated in correspondence of a value of temperature greater than 75 °C.

The situation depicted in Fig. 8 was always observed for all the cloudless days in which the measurements of the Sanyo panel were taken. Conversely, a very small difference between the measured and calculated data was observed for the Kyocera panel even if the same set of instruments were used.

Many may be the reasons of the observed differences between the issued, measured and calculated data. At first, in order to investigate the cause of the differences, the influence of the solar spectral irradiance was analysed using the air mass function [24,25] that permits to correct the short circuit current of the PV panel:

$$I_{sc}(AM) = I_{sc,ref}\ \alpha_G f(AM_a) \tag{8}$$

where absolute air mass AM_a is calculated with the expression:

$$AM_a = [\cos(Z_s) + 0.5057 \cdot (96.080 - Z_s)^{-1.634}]^{-1} \times e^{(-0.000118\ h)} \tag{9}$$

in which Z_s is the solar zenith angle and h is the site altitude in metres.The following expression was used to evaluate the air mass function:

$$f(AM_a) = a_0 + a_1 \times AM_a + a_2 \times AM_a^2 + a_3 \times AM_a^3 + a_4 \times AM_a^4 + a_5 \times AM_a^5 + a_6 \times AM_a^6 \tag{10}$$

with:

$$a_0 = 0.96055$$
$$a_1 = 3.23395 \times 10^{-2}, \quad a_2 = -3.94604 \times 10^{-3},$$
$$a_3 = 2.29220 \times 10^{-4}$$
$$a_4 = -6.84265 \times 10^{-6}, \quad a_5 = 1.01288 \times 10^{-7},$$
$$a_6 = -5.88530 \times 10^{-10}$$

The above coefficients were extracted from [24]. Because short circuit current I_{sc} is almost equal to photocurrent I_L, Eq. 8 was used to correct Eq. 3. As is shown in Figs. 8 and 9, even if the absolute air mass significantly varies during the day, the effect on the physical behaviour of the PV panel is irrelevant and consequently the observed differences between measured and calculated data cannot be mainly due to the solar spectral irradiance.

If no important phenomenon was omitted by the model, one may infer that the instruments were inaccurate and consequently

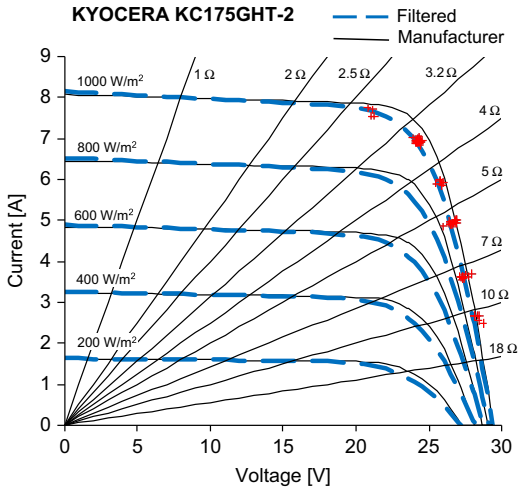

Fig. 11. Comparison between calculated with the filtered data and issued current–voltage characteristics of Kyocera KC175GHT-2 at temperature $T=25$ °C.

the true values of irradiance, temperature and voltage are different from the measured ones. In Table 5 the uncertainties of the measurements are presented.

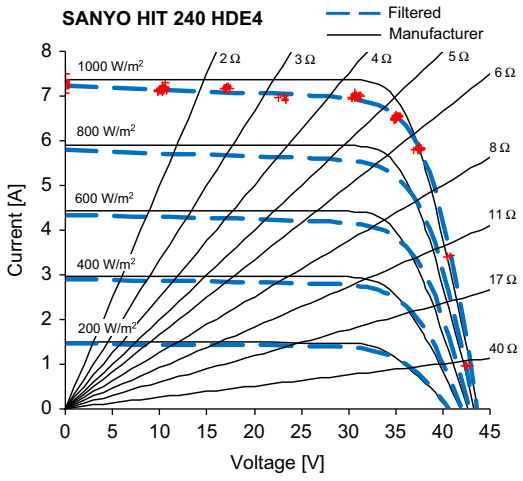

Fig. 12. Comparison between calculated with the filtered data and issued current–voltage characteristics of Sanyo HIT 240 HDE4 at temperature $T=25$ °C.

Actually, because in the observed operating point the sensitivity of the panel to the temperature is quite small, the difference should be mainly ascribed to the measurement of the irradiance. Unfortunately, because the uncertainty of the solar irradiance measurement, the observed difference between measured and calculated data and the tolerance declared by the manufacturer have the same order of magnitude and no unfailing opinion about the origin of the observed differences can be expressed.

On the other hand, it was observed that the difference between the measured and the calculated power was always negative for the Sanyo panel and consequently a kind of bias error of the instrument may be suspected. But, if the pyranometer was affected by a bias error, how to explain that for the Kyocera panel much smaller differences between the measured and the calculated power were always registered by the same instrument? Why the same pyranometer should be repeatedly imprecise only when the Sanyo panel is tested?

To answer these questions one may infer that the observed incoherence may be due to the tested PV panels; probably one of the tested panels does not perfectly comply with the current–voltage characteristics issued by the manufacturer. Following this idea, we tried to reconstruct the "true" current–voltage characteristics of the tested panel specimens in order to find the way to see if the model, which was built using only the information related to the STC, was able to describe the physical behaviour of the tested PV panels when they operate in more realistic conditions that are far from the few values of solar irradiance and operating temperature in correspondence of which IEC Standards bind manufactures to measure the panel electrical characteristics.

To reach the purpose all recorded data were filtered in order to select the measurements related to the values of the irradiance contained in the $\pm 1\%$ range around 1000 W/m^2. The filtered data were translated to the STC ($G_{ref}=1000$ W/m^2 and $T_{ref}=25$°C) by means of the following equations:

$$I(G_{ref},T_{ref}) = \frac{G_{ref}}{G} I(G,T) - \mu_{I,sc}(T-T_{ref}) \tag{11}$$

$$V(G_{ref},T_{ref}) = \frac{G_{ref}}{G} V(G,T) - \mu_{V,oc}(T-T_{ref}) \tag{12}$$

Table 6
Data for the evaluation of the model parameters for the filtered characteristics.

Irradiance	1 kW/m^2								0.2 kW/m^2
Temperature	25 °C						25–75 °C		25 °C
Panel type	V_{oc} [V]	I_{sc} [A]	V_{mp} [V]	I_{mp} [A]	R_{sho} [Ω]	R_{so} [Ω]	$\mu_{V,oc}$ [V/°C]	$\mu_{I,sc}$ [A/°C]	V_{oc} [V]
Kyocera KC175GHT-2	29.35	8.15	23.70	7.10	55.00	0.480	-1.07×10^{-1}	2.22×10^{-3}	27.20
Sanyo HIP-240 HDE4	43.60	7.22	34.40	6.65	120.00	0.700	-1.09×10^{-1}	2.12×10^{-3}	40.61

Table 7
Parameters of the model calculated for the filtered characteristics.

Irradiance	1 kW/m^2						0.2 kW/m^2
Temperature	25 °C					25÷75 °C	25 °C
Panel type	I_L [A]	I_0 [A]	n [V/K]	R_{sh}[Ω]	R_s[Ω]	K [Ω/°C]	I_0 [A]
Kyocera KC175GHT-2	8.19114	7.00144×10^{-9}	4.72988×10^{-3}	54.704	0.296	1	6.46493×10^{-9}
Sanyo HIP-240 HDE4	7.24436	3.79953×10^{-9}	6.86003×10^{-3}	119.597	0.403	1	3.29018×10^{-9}

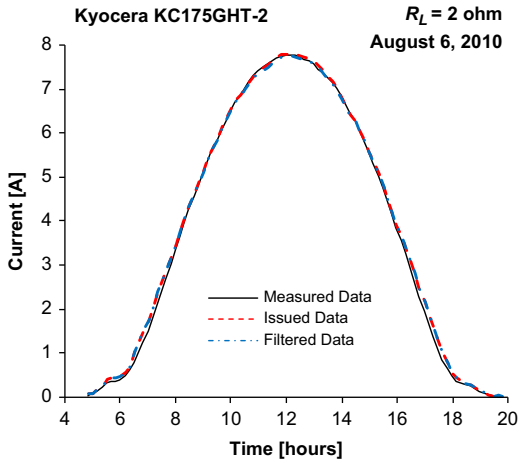

Fig. 13. Current of the PV module Kyocera KC175GHT-2 measured with an electrical load of 2 Ω versus the current evaluated with the issued and the filtered data.

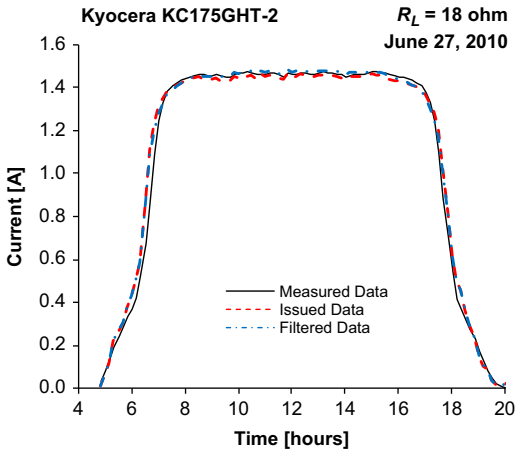

Fig. 16. Current of the PV module Kyocera KC175GHT-2 measured with an electrical load of 18 Ω versus the current evaluated with the issued and the filtered data.

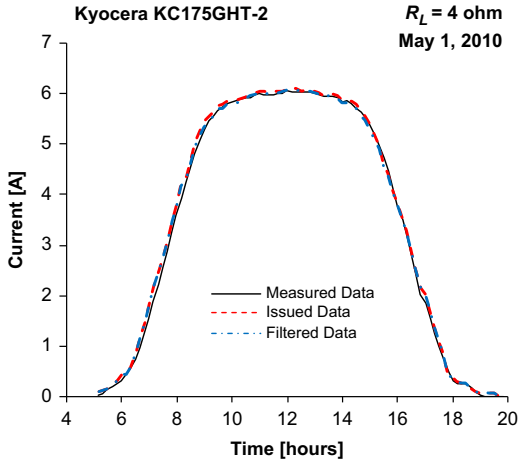

Fig. 14. Current of the PV module Kyocera KC175GHT-2 measured with an electrical load of 4 Ω versus the current evaluated with the issued and the filtered data.

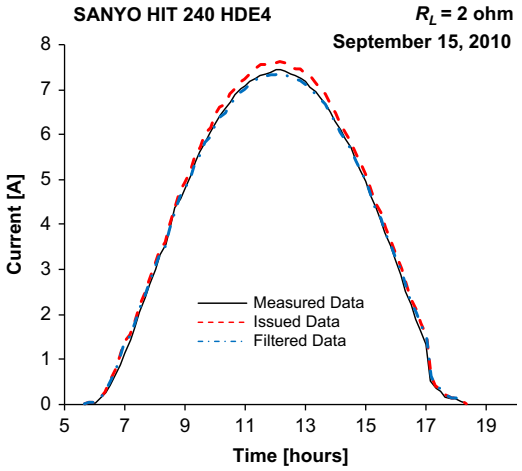

Fig. 17. Current of the PV module Sanyo HIT 240 HDE4 measured with an electrical load of 2 Ω versus the current evaluated with the issued and the filtered data.

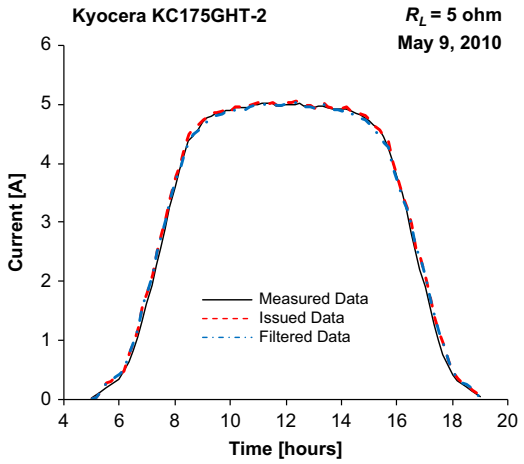

Fig. 15. Current of the PV module Kyocera KC175GHT-2 measured with an electrical load of 5 Ω versus the current evaluated with the issued and the filtered data.

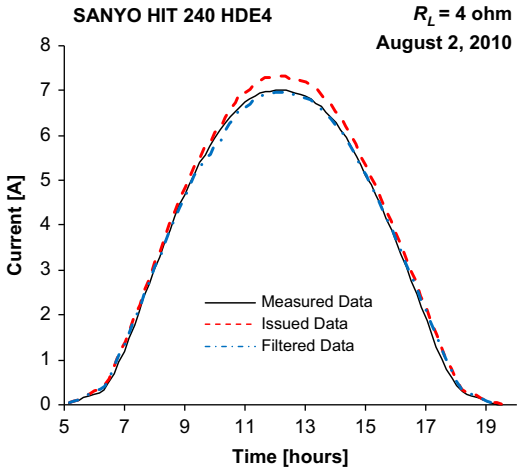

Fig. 18. Current of the PV module Sanyo HIT 240 HDE4 measured with an electrical load of 4 Ω versus the current evaluated with the issued and the filtered data.

that can be considered adequate for the very small difference in the values of irradiance.

The translated data, which are indicated with small crosses in Figs. 11 and 12, were used to estimate the parameters of the "true" I–V characteristic at STC that are necessary to calculate the Lo Brano et al. model. The data for the evaluation of the Lo Brano et al. model and the calculated values of the parameters are listed in Tables 6 and 7. As it was described in [6], thermal correction factor K can be calculated using the values of V^*_{mp} and I^*_{mp}, which are the coordinates of the maximum power point on the issued characteristic at $T \neq 25$ °C. Because the values of V^*_{mp} and I^*_{mp} on the "true" I–V characteristic at $T \neq 25$ °C were unknown, it was assumed $K=1$.

The results of the procedure are shown in Figs. 11 and 12. It is easy to observe that the "true" I–V characteristics are rather different from the curves issued by the manufacturers; the electrical performances of the PV panels seem to be worsened, especially for the Sanyo PV panel.

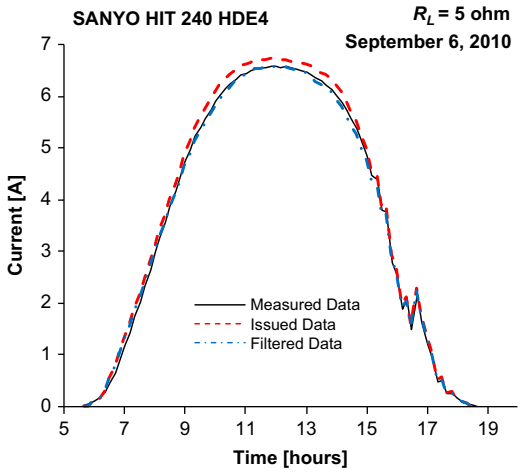

Fig. 19. Current of the PV module Sanyo HIT 240 HDE4 measured with an electrical load of 5 Ω versus the current evaluated with the issued and the filtered data.

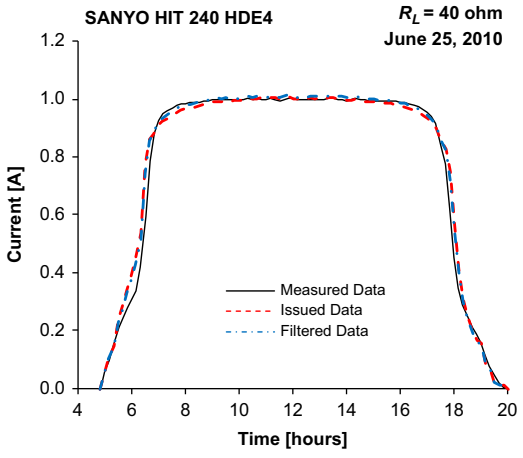

Fig. 20. Current of the PV module Sanyo HIT 240 HDE4 measured with an electrical load of 40 Ω versus the current evaluated with the issued and the filtered data.

4. Results and discussion

The results of predictions of the operating current and power from the Lo Brano et al. model were analysed for each value of the connected electrical loads using meteorological data-sets consisting of one-day long data, from sunrise to sunset. According to the permitted weather conditions, in order to examine the panels working in almost steady-state conditions only the data-sets of the sunniest days were used. As it is depicted in Fig. 19, where the discontinuities occurred at 16:00 were due to the inopportune passage of few clouds due to the specific weather conditions of September, sometimes it was impossible to perform the measurements in quite perfect cloudless days. In those days the irradiance on the panel planes reached a maximum value of about 1000 W/m^2 and the silicon temperature varied on average between 20 and 50 °C. The results of the comparison between measured and calculated data are shown in Figs. 13–20; for the sake of brevity, for each PV panel only the most significant graphs were reported.

Figs. 13–20 show the good agreement between the measured current and the current calculated with the Lo Brano et al. model. In particular the quality of the calculations is improved by using the model based on the "true" I–V characteristics of the tested PV panels. Tables 8 and 9 present, for all values of the used electrical loads, some accuracy figures of the comparison between the measurements and the calculations performed with the Lo Brano et al. model based on the data related to the "true" I–V characteristics of the tested silicon PV panels.

The results of the experimental validation can be considered satisfactory. For the Kyocera PV panel the maximum value of the power mean difference (−1.635 W) is −0.93% of the declared nominal power (175 W). The maximum error in the estimate of the electricity collected during the day is 1.67%. Even the daily mean efficiency of the PV panel is accurately evaluated. The Sanyo PV shows a maximum value of the power mean difference (−7.906 W) that is −3.29% of the declared nominal power (240 W). The maximum error in the estimate of the electricity collected during the day is 4.31% and the daily mean efficiency of

Table 8
Accuracy figures from the experimental validation of the Lo Brano et al. model with the Kyocera KC175GHT-2 PV panel.

Data-set	R_L [Ω]	Mean difference		Daily collected energy [kJ]				Daily Efficiency [%]		
		Current [A]	Power [W]	Meas.	Calc.	Error [%]	Solar	Meas.	Calc.	Error [%]
Jun. 16/10	1.0	0.023	0.165	1,179	1,181	−0.14	32,537	3.62	3.63	−0.28
Jun. 08/10	2.0	0.049	−0.291	2,529	2,545	0.63	34,258	7.38	7.43	−0.67
Jun. 06/10	2.5	0.047	−1.072	3,136	3,150	0.44	34,530	9.08	9.12	−0.44
May 26/10	3.2	0.032	−1.635	3,751	3,762	0.31	35,497	10.57	10.60	−0.28
May 01/10	4.0	0.052	−1.596	3,829	3,876	1.22	35,996	10.64	10.77	−1.21
May 09/10	5.0	0.033	−1.136	3,626	3,640	0.40	35,738	10.15	10.19	−0.39
Jun. 28/11	7.0	0.037	0.275	2,811	2,858	1.67	33,335	8.43	8.57	−1.63
Apr. 03/10	10.0	0.027	−0.246	2,435	2,450	0.59	35,987	6.77	6.81	−0.59
Jun. 27/10	18.0	0.013	0.353	1,494	1,508	0.96	34,042	4.39	4.43	−0.90

Table 9
Accuracy figures from the experimental validation of the Lo Brano et al. model with the Sanyo HIT 240 HDE4 PV panel.

Data-set	R_L [Ω]	Mean Difference		Daily collected energy [kJ]				Daily efficiency [%]		
		Current [A]	Power [W]	Meas.	Calc.	Error [%]	Solar	Meas.	Calc.	Error [%]
Sep. 15/10	2.0	−0.009	−3.292	2,195	2,167	−1.25	36,539	6.01	5.93	1.35
Jun. 06/10	3.0	0.112	−4.792	2,981	3,109	4.31	37,480	7.95	8.30	−4.22
Aug. 02/10	4.0	0.008	−7.906	4,199	4,145	−1.30	37,603	11.17	11.02	1.36
Sep. 06/10	5.0	−0.006	−7.646	4,735	4,682	−1.12	35,851	13.21	13.06	1.15
Jul. 28/10	6.0	0.027	4.206	5,081	5,082	0.02	37,692	13.48	13.48	0.00
Jun. 17/10	8.0	0.027	1.374	4,605	4,613	0.18	36,333	12.67	12.70	−0.24
Jul. 23/10	11.0	0.011	0.172	3,957	3,950	−0.17	35,659	11.10	11.08	0.18
Aug. 08/10	17.0	0.033	0.668	3,115	3,185	2.26	37,185	8.38	8.57	−2.22
Jun. 25/10	40.0	0.011	0.347	1,594	1,628	2.14	37,599	4.24	4.33	−2.08

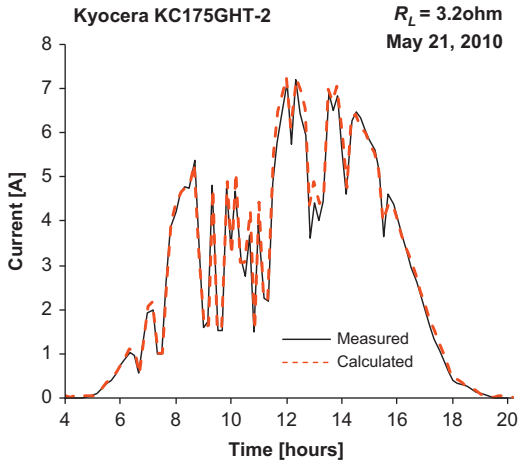

Fig. 21. Current of the PV module Kyocera KC175GHT-2 measured with an electrical load of 4 Ω on May 21, 2010 versus the current calculated with the Lo Brano et al. model.

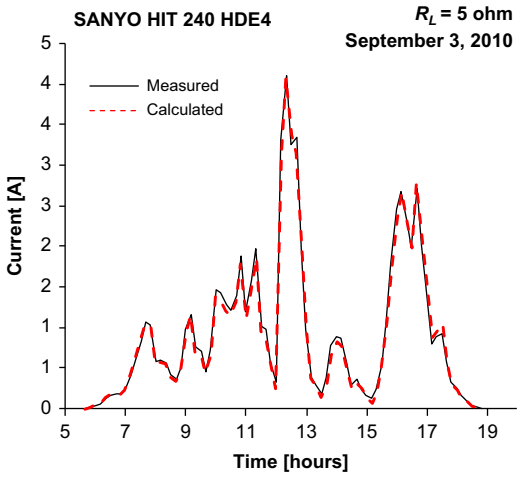

Fig. 23. Current of the PV module Sanyo HIT 240 HDE4 measured with an electrical load of 4 Ω on September 3, 2010 versus the current calculated with the Lo Brano et al. model.

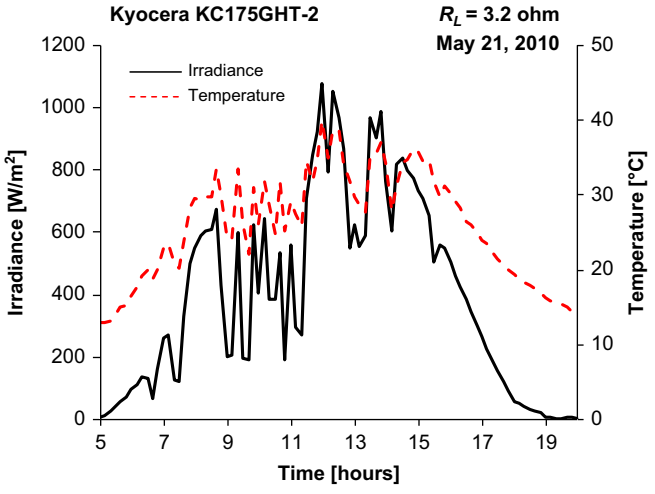

Fig. 22. Irradiance and PV panel temperature measured on May 21, 2010.

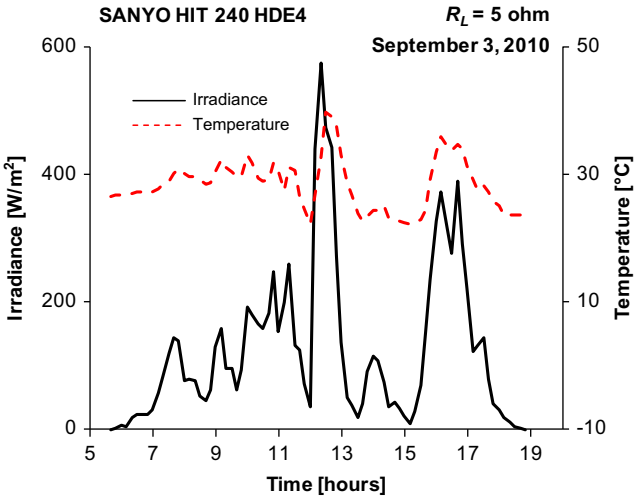

Fig. 24. Irradiance and PV panel temperature measured on September 3, 2010.

the PV panel is accurately evaluated. Obviously the above accuracy parameters are related to the value of the current calculated from the voltage drop measured on the resistance R_L whose value is known with a declared tolerance range of ± 1.625%.

Even though the "true" characteristics were identified for the irradiance of 1000 W/m^2 and the temperature of 25 °C, the model is able to accurately predict the electrical behaviour of the tested PV panels in correspondence of values of irradiance and temperature far from the STC. The capability of the Lo Brano et al. model to adequately represent the electrical behaviour of silicon PV panels in all conditions is confirmed in Figs. 21–24 where the data refer to days when the irradiation and the panel temperature irregularly varied.

Eventually, it must be observed that the "true" I–V characteristics of the tested PV panels were obtained by simply interpolating the electrical data measured in the field in non-steady

conditions; probably, if the performance data of each PV panel were acquired with laboratory measurements, the validated model would demonstrate a better accuracy.

5. Conclusions

In order to validate a predictive tool by comparing the measured data with the results of analytical computations it is necessary that the declared performance data of the studied system, which are used to define the tool parameters, correspond to the actual physical behaviour of the system. Because the technology of silicon devices does not permit to keep a small production spread, the comparison between the data measured on a single PV panel and those calculated with an equivalent electrical circuit may led to inconsistent conclusions. Actually the performance characteristics of the tested specimen should be used to set the parameters of the equivalent circuit; such a need requires many painstaking laboratory measurements.

To perform an experimental validation in the field the silicon PV panels were connected to nine different load resistances selected in order to widely explore the I–V characteristics. At first the parameters of the Lo Brano et al. model were calculated using the characteristics provided by the manufacturers. Despite the high accuracy with which the model was able to calculate the issued I–V curves, the comparisons with the data measured on the tested specimens of Kyocera and Sanyo PV panels resulted unsatisfactory. A further analysis on the correspondence between measure and issued data highlighted some aspects of inconsistency of the provided I–V characteristics.

Using the experimental data collected when the irradiance was close to the values of the STC, a new "true" I–V characteristic was determined for both silicon PV panels and such a characteristic was used to evaluate the parameters of the Lo Brano et al. model. The results of the comparisons between the measured current and the values calculated with the model on the basis of the "true" characteristics, resulted very satisfactorily. The model has also shown the capability to accurately predict the electrical performances of the silicon PV panels during days perturbed by very variable conditions of solar irradiance.

References

[1] W. De Soto, S.A. Klein, W.A. Beckman, Improvement and validation of a model for photovoltaic array performance, Solar Energy 80 (2006) 78–88.
[2] T.U. Townsend A Method for Estimating the Long-Term Performance of Direct-Coupled Photovoltaic Systems, M.Sc. thesis, Mechanical Engineering, University of Wisconsin-Madison, (1989).
[3] M.A. de Blas, J.L. Torres, E. Prieto, A. Garcia, Selecting a suitable model for characterizing photovoltaic devices, Renewable Energy 25 (2002) 371–380.
[4] A.N. Celik, N. Acikgoz, Modelling and experimental verification of the operating current of mono-crystalline photovoltaic modules using four-and five-parameter models, Applied Energy 84 (2007) 1–15.
[5] A. Hadj Arab, F. Chenlo, M. Benghanem, Loss-of-load probability of photovoltaic water pumping systems, Solar Energy 76 (2004) 713–723.
[6] V. Lo Brano, A. Orioli, G. Ciulla, A. Di Gangi, An improved five-parameter model for photovoltaic modules, Solar Energy Materials & Solar Cells 94 (2010) 1358–1370.
[7] M. Wolf, H. Rauscenbach, Series resistance effects on solar cell measurements, Advanced Energy Conversion 3 (1963) 455–479.
[8] T. Markvart, L. Costañer, Solar Cells. Materials, Manufacture and Operation, Elsevier, Oxford, 2005.
[9] PVsyst, Software for Photovoltsic Sysytems, University of Geneva ISE—Group Energy, FOREL Battelle, bât. D7, Route de Drize, CH-1227 Carouge, Switzerland.
[10] T.K. Mallick, P.C. Eames, T.J. Hyde, B. Norton, The design and experimental characterisation of an asymmetric compound parabolic photovoltaic concentrator for building facade integration in the UK, Solar Energy 77 (2004) 319–327.
[11] C.S. Sangani, C.S. Solanki, Experimental evaluation of V-trough (2 suns) PV concentrator system using commercial PV modules, Solar Energy Materials & Solar Cells 91 (2007) 453–459.
[12] N. Hamrouni, M. Jraidi, A. Chérif, Theoretical and experimental analysis of the behaviour of a photovoltaic pumping system, Solar Energy 83 (2009) 1335–1344.
[13] J.K. Kaldellis, E. Meidanis, D. Zafirakis, Experimental energy analysis of a stand-alone photovoltaic-based water pumping installation, Applied Energy 88 (2011) 4556–4562.
[14] T.T. Chow, W. He, J. Ji, An experimental study of facade-integrated photovoltaic/water-heating system, Applied Thermal Engineering 27 (2007) 37–45.
[15] T.T. Chow, W. He, A.L.S. Chan, K.F. Fong, Z. Lin, J. Ji, Computer modeling and experimental validation of a building-integrated photovoltaic and water heating system, Applied Thermal Engineering 28 (2008) 1356–1364.
[16] E. Erdil, M. Ilkan, F. Egelioglu, An experimental study on energy generation with a photovoltaic (PV)—solarthermal hybrid system, Energy 33 (2008) 1241–1245.
[17] K. Touafek, M. Haddadi, A. Malek, Experimental study on a new hybrid photovoltaic thermal collector, Applied Solar Energy 45 (2009) 181–186.
[18] C.D. Corbin, Z.J. Zhai, Experimental and numerical investigation on thermal and electrical performance of a building integrated photovoltaic–thermal collector system, Energy and Buildings 42 (2010) 76–82.
[19] J. Ji, G. Pei, T. Chow, K. Liu, H. He, J. Lu, C. Han, Experimental study of photovoltaic solar assisted heat pump system, Solar Energy 82 (2008) 43–52.
[20] F. Guiyin, H. Hainan, L. Xu, Experimental investigation on the photovoltaic–thermal solar heat pump air-conditioning system on water-heating mode, Experimental Thermal and Fluid Science 34 (2010) 736–743.
[21] H. Chen, S.B. Riffat, Y. Fu, Experimental study on a hybrid photovoltaic/heat pump system, Applied Thermal Engineering 31 (2011) 4132–4138.
[22] E. Román, V. Martinez, J.C. Jimeno, R. Alonso, P. Ibañez, S. Elorduizapatarietxe, Experimental results of controlled PV module for building integrated PV systems, Solar Energy 82 (2008) 471–480.
[23] A.H. Fanney, B.P. Dougherty, M.W. Davis, Evaluating Building Integrated Photovoltaic Performance Models, Proceedings of the 29th IEEE Photovoltaic Specialists Conference (PVSC), May 20–24, 2002, New Orleans, LA.
[24] D.L. King, J.A. Kratochvil, W.E. Boyson, Measuring Spectral and Angle-of-Incidence Effects on Photovoltaic Modules and Solar Irradiance Sensors, 26th IEEE Photovoltaic Specialists Conference, September 29–October 3, 1997, Anaheim, CA.
[25] D.L. King, W.E. Boyson, J.A. Kratochvil, Photovoltaic array performance model, August 2004, Photovolatic Systems R&D Department, Sandia National Laboratories, Albuquerque, New Mexico.